doi:10.3788/gzxb20184703.0301002

机载激光测深雷达中大动态范围信号的多通道处理技术

李杰[1,2],赵毅强[1,2],叶茂[1,3],胡凯[1,2],谢绍禹[1],薛文佳[1,2],周国清[1]

(1 天津大学 微电子学院,天津 300072)

(2 天津市成像与感知微电子技术重点实验室,天津 300072)

(3 天津市红外成像技术工程中心,天津 300072)

摘 要:为实现大动态范围信号的有效接收,设计了一种三路并行的信号处理架构,分别设置为低、中、高三种不同增益,以实现不同水深下不同幅度的回波信号处理.同时利用数据拼接方法以及一种基于五角函数和高斯函数组合的拟合算法综合处理三路数据并进行水深评估.基于 Wa-LID 回波仿真模型得到回波数据,验证多路并行处理架构的实用性.仿真结果表明,本文提出的多通道处理技术可测信号的动态范围达 86.9 dB,对应的最大测深为 26 m,测量偏差为 1.6 cm 至 4.7 cm,标准差小于 1.1 cm.可有效应用于机载激光雷达测深系统.

关键词:激光雷达;海洋测深学;多通道;回波;大动态范围;数据拼接方法;拟合算法

中图分类号:TN958.98 **文献标识码**:A **文章编号**:1004-4213(2018)03-0301002-7

Multi-channel Processing Technology for Wide Dynamic Range Signal in Airborne Lidar Bathymetry

LI Jie[1,2], ZHAO Yi-qiang[1,2], YE Mao[1,3], HU Kai[1,2],
XIE Shao-yu[1], XUE Wen-jia[1,2], ZHOU Guo-qing[1]

(1 *The School of Microelectronics, Tianjin University, Tianjin* 300072, *China*)

(2 *Tianjin Key Laboratory of Imaging and Sensing Microelectronic Technology, Tianjin* 300072, *China*)

(3 *Tianjin Infrared Imaging Technology Engineering Center, Tianjin* 300072, *China*)

Abstract: Three-channel processing structure was proposed to extend the input dynamic range. Each channel is set up with low, middle or high gain according to the echo intensity from different water depth. Afterwards, a data stitching method and a new fitting approach with the combination of pentagonal and Gaussian function are applied to each three-channel waveform to estimate the depth of water. The multi-channel processing structure was verified on the simulated data sets obtained from the existing Wa-LID waveform simulator. The simulated result has shown that the effective input signal is up to 86.9 dB dynamic range in this new processing technique, and the measured depth reaches 26 m. The bias of the bathymetry estimates is ranging from 1.6 to 4.7 cm with the standard deviation better than 1.1 cm. This multi-channel processing technology can be effectively used in ALB.

Key words: Lidar; Bathymetry; Multi-channel; Echo; Wide dynamic range; Data stitching method;

Foundation item: State Oceanic Administration of China under Grant CaiJianHan (No.58) and Tianjin Science and Technology Project of China(No.15ZCZDGX00180)

First author: LI Jie (1992—), male, M.S.degree candidate, mainly focuses on data acquisition and processing of Airborne lidar. Email:jack_li@tju.edu.cn

Supervisor (Contact author): ZHAO Yi-qiang (1964—), male, professor, Ph.D. degree, mainly focuses on photoelectric detection. Email: yq_zhao@tju.edu.cn

Received: Aug. 21, 2017; **Accepted**: Nov. 23, 2017

Fitting algorithm
OCIS Codes: 010.3640; 280.1355; 280.3640; 010.4450; 040.5160; 070.1170

0 Introduction

Airborne Lidar Bathymetry (ALB) is an accurate, cost-effective and efficient technique for shallow water measurements. As the laser pulse travels through the water column and encounters the bottom of sea, it undergoes absorption, scattering and refraction. These processes attenuate the laser return energy, ultimately limiting the depth at which sea bottom can be detected[1-3].

In general, the return signal reflected from the water column varies dramatically with water depth[4]. Therefore, the common survey system prepares two bottom detecting receiving channels, such as the SHOALS system, which equips two receiving channels measuring the green laser return from shallow water depths, 1～12 m, and intermediate water depths, 7～40 m[5]. Actually, the Photomultiplier Tube (PMT) of Hamamatsu, H1156-20-NN, exhibits typical dark current of 10 nA, while the max output current reaches 100 μA. The dynamic range of the PMT[6-7] is calculated by DRPMT = 20 × lg(100 μA/10 nA) = 80 dB.

However, the available maximum dynamic range of a typical high-speed 8 bit Analog to Digital Converter (ADC) device is 48.16 dB. Therefore, it is impossible to process the signal received aptly all the time even though the noise level is not considered.

For the HawkEye II system, the received signal from the two green channel receivers is applied with a Time-Varied Gain (TVG) filter to enhance the bottom return [8].However, it would cause the problem of waveform distortion. Moreover, on account of bottom radiance and water turbidity[9-12], the amplitude of bottom return is variable and unknown[13], so it is not impeccable to only depend on optical attenuation or gain adjustment.

In this paper, we aim to design a new processing structure to receive the signal with 80 dB dynamic range and verify the reliability of the design by waveform stitching method and fitting algorithm, along with the objective of making the entire predictive system more accurate.

1 Materials and methods

1.1 Waveform simulation

The waveform data set is generated by using the recently developed Wa-LID simulator[14], which is the summation of the laser pulse convolution with the impulse response functions of the surface, column and bottom, as well as additional noises. In our simulations, the partial values of system parameters acting in the Wa-LiD equations and partial environment parameters are listed in Table 1 and Table 2, respectively.

Table 1 System parameters

Parameters	Value
Laser wavelength/ nm	532
Emitted energy/ mJ	3
Pulse width/ns	5
Digitizing frequency/GHz	2
Quantization bits/bit	8
Incidence angle/(°)	10
Emitted optical efficiency	0.9
Receiver optical efficiency	0.5
Instantaneous field of view/sr	1.1×10^{-5}
Spectral filter bandpass/nm	1
Solar radiance/($W\cdot m^{-2}sr^{-1}$)	0.025
Electrical bandwidth/MHz)	200
Detector responsivity/($A\cdot W^{-1}$)	1.5×10^{5}
Dark current/A	1×10^{-8}

Table 2 Range of environment parameters

Parameters	Range values
Two-way atmospheric loss	0.9
Surface roughness	0.24
Concentration of yellow substances/ m^{-1}	0.014
Concentration ofphytoplankton/($\mu g \cdot L^{-1}$)	0.237
Concentration of sediments/($mg \cdot L^{-1}$)	1
Bottom albedo	0.2
Specularreflection	0.9

In order to compute accuracy statistics on the bathymetry estimates, the data set is generated. Data set contains 1000 simulated waveforms for each water depth.

1.2 Design and analysis of three-channel processing structure

In order to receive a signal with 80 dB dynamic range, a three-channel processing structure illustrated in Fig. 1 has been introduced into the design.

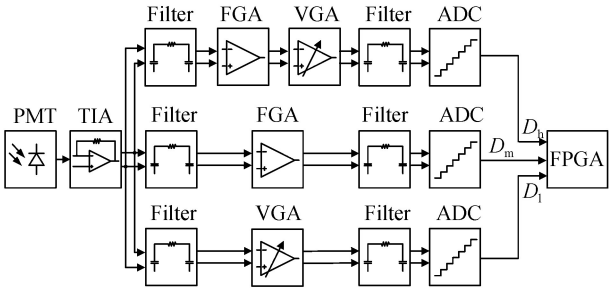

Fig.1 Three-channel processing structure

PMT with high sensitivity is used to record the return signal events and process the return signal in conjunction with the three-channel processing structure. Here, we use the Trans-impedance Amplifier (TIA) and the filter to pre-process the return . Afterwards , the strong signal (shallow water returns), the middle signal (intermediate water returns) and the weak signal (deeper returns) with low, middle and high gain in parallel processing mode are amplified, respectively, by utilizinga Variable - Gain Amplifier (VGA) , a Fixed - Gain Amplifier (FGA) and the combination of the two. The D_l, D_m and D_h are the data sampled by the high-speed ADC in the low, middle and high gain channel respectively, finally captured by Field Programmable Gate Array(FPGA).

In this paper, we set low gain $G_l=1$, middle gain $G_m=10$ and high gain $G_h=100$, which could achieve dynamic range of 88.1 ($20\times\lg(256\times G_h)$) dB theoretically. The three-channel waveform at the depth of 18 m quantified by ADC is illustrated in Fig. 2. The ADC used in the structure is a 2GSPS, 8 bit device. The horizontal axis in Fig.2 is the number of sample points and the vertical axis is the output code from the ADC.

In Fig. 2, it is appropriate that the bottom return is amplified by high gain channel obviously.

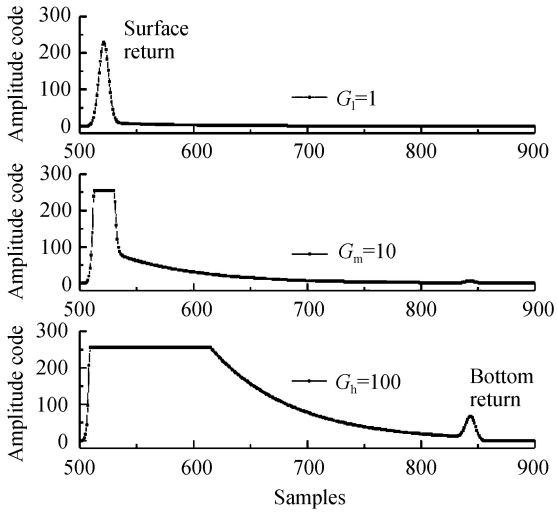

Fig.2 Three-channel waveform with different gains

1.3 Bathymetry estimation from three-channel waveform

For the purpose of utilizing the waveforms recorded by the design preferably, the three-channel simultaneous recordings are stitched. The stitching method is given by

$$D=\begin{cases} D_l+D_m+D_h & (D_h=2.\wedge Q_b-1, D_m=2.\wedge Q_b-1) \\ D_m+D_h & (D_h=2.\wedge Q_b-1, D_m<2.\wedge Q_b-1) \\ D_h & (D_h<2.\wedge Q_b-1) \end{cases} \quad (1)$$

where Q_b is quantization bits, D is the data sets after stitching. Furthermore, there are advantages of keeping the correlation among the waveform data in this process and avoiding the problem of waveform distortion existing in the system which uses the TVG filter.

After stitching and smoothing, apeak detection procedure is used on the smoothed waveforms. It

regards a peak as any local maxima in the lidar waveform that has an amplitude much higher than the noise level, 8 times in this paper. Thus, the dynamic range limited by peak detection is changed to 70.0 dB (88.1-20lg (8)).

The peak with the largest amplitude is attributed to the surface position (A_s,μ_s) while the peak with the largest time is attributed to the bottom position (A_b, μ_b). After peak detection, the fitting procedure is applied to the waveforms that have a detectable bottom. The pentagonal function is used to fit the water column contribution on account of the different slopes in column return caused by different gains. The surface and bottom returns are considered to be Gaussian functions. So the fitted lidar waveform can be expressed as

$$R(t)=G(t;A_s,\mu_s,\sigma_s)+Q(t;a,b,c,d,e,g,h,f)+G(t;A_b,\mu_b,\sigma_b) \tag{2}$$

where G (t; A_s, μ_s, σ_s) is the Gaussian function defined as

$$G(t;A_s,\mu_s,\sigma_s)=A_s\exp\left(-(t-\mu_s)^2/2\sigma_s^2\right) \tag{3}$$

where A_s, μ_s, and σ_s are the amplitude, the mean and the standard deviation of the Gaussian function, respectively.

The Q (t; a, b, c, d, e, g, h, f) is given by

$$Q(t;a,b,c,d,e,g,h,f)=\begin{cases}0 & (t\leqslant a)\\ e((t-a)/(b-a)) & (a\leqslant t\leqslant b)\\ [ec-bg+t(g-e)]/(c-b) & (b\leqslant t\leqslant c)\\ [gd-hc+t(h-g)]/(d-c) & (c\leqslant t\leqslant d)\\ h((f-t)/(f-d)) & (d\leqslant t\leqslant f)\\ 0 & (t\geqslant f)\end{cases} \tag{4}$$

where a, b, c, d, and f are the x-axis points of five corners for the pentagonal; and e, g, and h are the ordinates for three vertices, respectively.

The G (t; A_b, μ_b, σ_b) is the Gaussian function defined as

$$G(t;A_b,\mu_b,\sigma_b)=A_b\exp\left(-(t-\mu_b)^2/2\sigma_b^2\right) \tag{5}$$

where A_b, μ_b, and σ_b are the amplitude, the mean and the standard deviation of the Gaussian function, respectively.

A Nonlinear Least-Squares (NLS) approach using the Levenberg-Marquardt optimization algorithm is performed to fit the sum of three functions. The initial values of NLS fitting are listed in Table 3, where T_0 is pulse width.

Table 3 Initial values of fitting

Parameters	Values	Parameters	Values
σ_s	$T_0/(8\ln 2)^{1/2}$	d	$(\mu_s+\mu_b)/2$
σ_b	$T_0/(2\ln 2)^{1/2}$	f	$(A_s+A_b)/2$
a	$\mu_s+2\sigma_s$	e	$A_s/2$
b	$\mu_s+3\sigma_s$	g	$A_b/2$
c	$\mu_s+10\sigma_s$	g	$\mu_b-3\sigma_b$

2 Results and discussion

In order to verify that the three-channel processing structure could enhance the bottom return and make the entire predictive system more accurate, some data sets are generated. Of the overall waveforms, the dynamic range DR_0, i.e., the ratios of the surface peak and the bottom peak is calculated. After simulation, it proves that the DR_0 exceeds 71.1 dB at water depths greater than 27 m, which is beyond the dynamic range limited by peak amplitude definition (70.0 dB). Thus, the dynamic range DR_0 at water depths of 1 m to 27 m are shown in Fig.3 (a), and the peak detection rates of the three-channel and the one-channel processing approach are shown in Fig.3 (b).

At the water depths of 1-26 m, the DR_0 reaches 68.9 dB, which means 86.9 dB (68.9+20lg (8)) for the received signal when the limit of peak detection taken into account. As a result, the advantage of the three - channel processing structure is evident . The bottom return can still be detected when water depth is

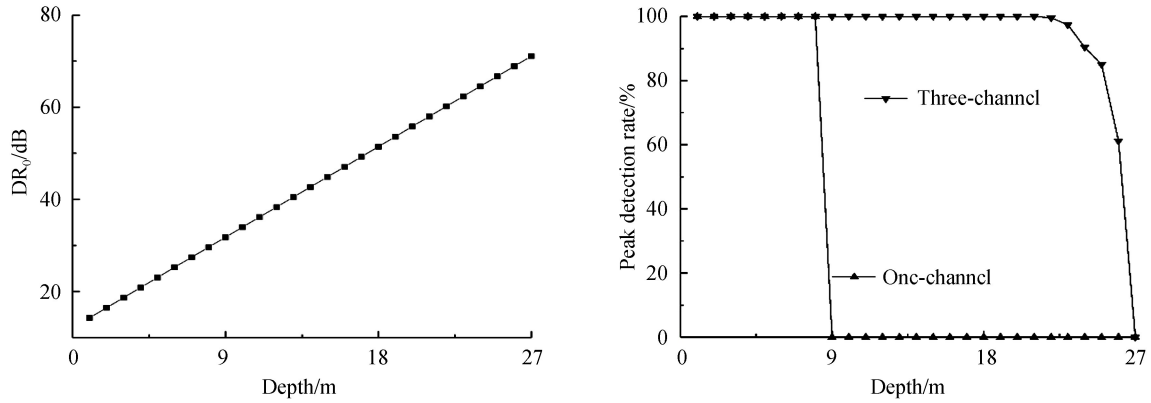

(a) The ratio of surface peak to bottom peak (b) The peak detection rate at each depth

Fig.3 The ratio of surface peak to bottom peak and the peak detection rate at each depth

greater than 8 m, at which the dynamic range reaches 29.6 dB, about 47.6 dB (29.6+20lg (8)) for the received signal, while the one-channel is out-of-range for the property.

The Signal to Noise Ratio (SNR) is calculated for each water depth, which is defined here by the ratio of the bottom peak amplitude in the waveforms to the noise amplitude. For the water depths of 1～26 m, the maximum SNRs of bottom return with a detectable bottom in three-channel are shown in Fig.4.

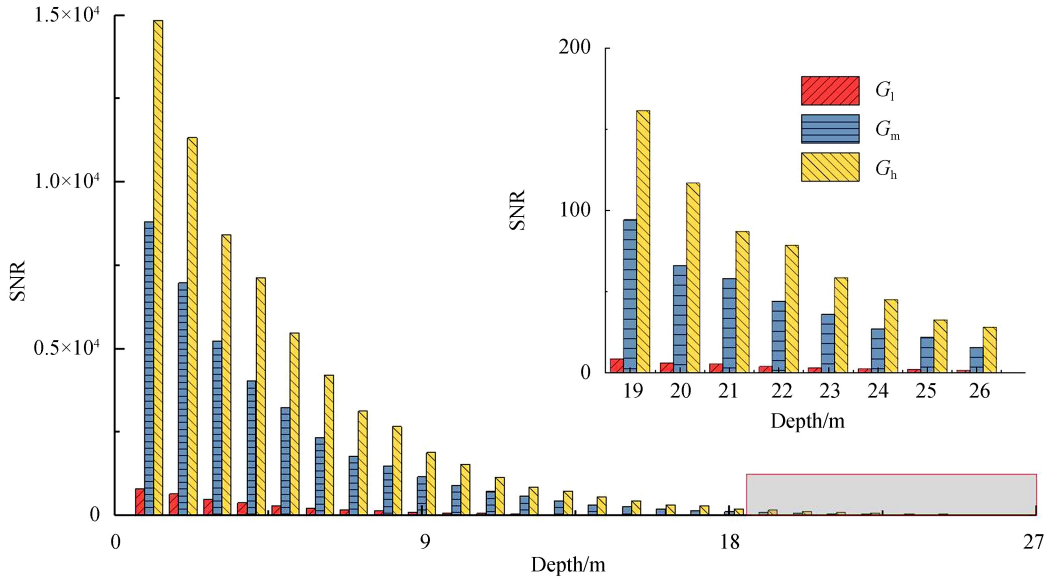

Fig.4 The SNRs for waveforms at the water depths of 1～26 m

In Fig.4, The maximum SNR decreases with water depth, which reduces from 804.2 at 1m water depth to 1.4 at 26 m water depth in low gain channel, from 8 808.7 to 15.7 in middle and from 14 851.6 to 28.2 in high.

By using the fitted parameter values, the bias, i.e., the mean difference betweenthe estimated and simulated water depths as well as the standard deviation of the bathymetry estimates are computed. The fitting results and the accuracy of fitting algorithm at water depths of 1 to 26 m are shown in Fig.5.

The simulation result shows that the bias ranges from 1.6 to 4.7 cm at water depths of 1 m to 26 m. Besides, the standard deviation is better than 1.1 cm. The overall bias and standard deviation for all the used water depths are shown in Table 4, as well as the results in Ref.[15] and Ref.[16].

The result of error statistics shows improvements of 2.7 cm in bias, 7.3 cm in standard deviation and 16 m for limiting depth compared with Ref.[15]. Additionally, it takes on superiority of 1.9 cm in standard deviation and 11 m for limiting depth compared with Ref.[16]. This proves that it is feasible to reach a greater dynamic range by using the three-channel processing structure which could achieve more accurate performance for bathymetry estimate and greater limiting depth.

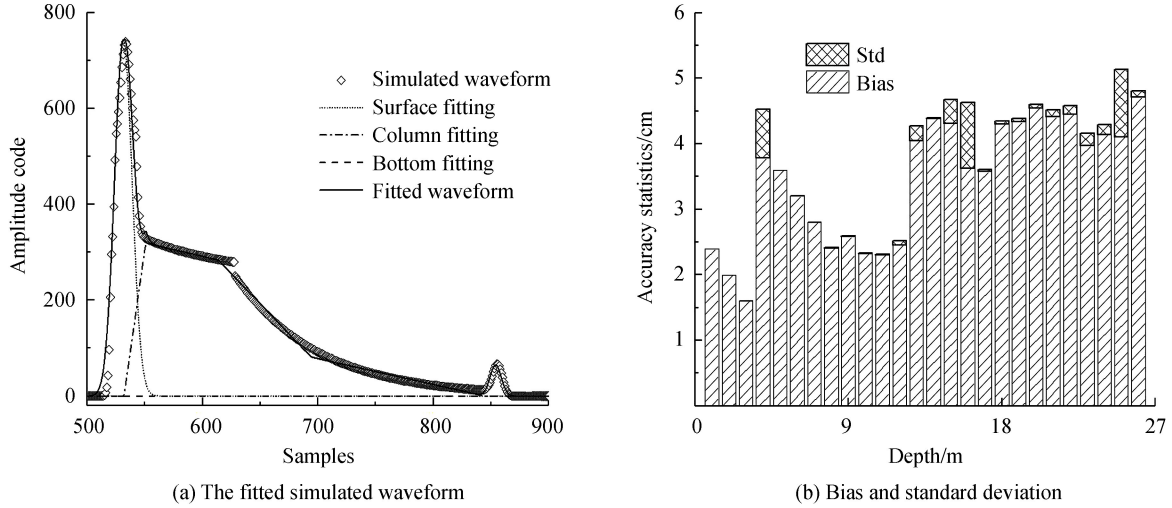

(a) The fitted simulated waveform (b) Bias and standard deviation

Fig.5 The fitted simulated waveform at water depth of 18 m, bias and standard deviation on bathymetry estimates

Table 4 Bathymetry accuracycompared with reference paper

	Max depth/m	Bias/cm	Std/cm	Detection rate/%
Proposed method	26	3.4	0.9	95.4
Ref.[15]	10	6.1	8.2	39.6
Ref.[16]	15	0.5	2.8	<63

3 Conclusion

In conclusion, we propose a novel processing structure and method to process the signal with 80 dB dynamic range and verify the reliability of bathymetry estimates through simulation and analysis. The result has shown that the processing structure could measure the echoes of water depth of 1 m to 26 m, with the dynamic range of 86.9 dB, better than 47.6 dB achieved by the one-channel. The bias of the bathymetry estimates is ranging from1.6 to 4.7 cm with the standard deviation better than 1.1 cm. This processing structure satisfies the requirement of receiving and processing the signal with a wide dynamic range in lidar bathymetry. We will continue to study various coastal areas to develop a practical and reliable method for bathymetry.

References

[1] BAILLY J S, LE COARER Y, LANGUILLE P, *et al*. Geostatistical estimations of bathymetric LiDAR errors on rivers [J]. *Earth Surface Processes and Landforms*, 2010, **35**(10): 1199-1210.

[2] PAN Z, GLENNIE C, HARTZELL P, *et al*. Performance assessment of high resolution airborne full waveform LiDAR for shallow river bathymetry[J]. *Remote Sensing*, 2015, **7**(5): 5133-5159.

[3] JASINSKI M F, STOLL J D, COOK W B, *et al*. Inland and near-shore water profiles derived from the high-altitude Multiple Altimeter Beam Experimental Lidar (MABEL)[J]. *Journal of Coastal Research*, 2016, **76**(sp1): 44-55.

[4] ZHAO J, ZHAO X, ZHANG H, *et al*. Improved model for depth bias correction in airborne LiDAR bathymetry systems[J]. *Remote Sensing*, 2017, **9**(7): 710.

[5] IRISH J L, MCCLUNG J K, LILLYCROP W J. Airborne lidar bathymetry: the SHOALS system[R]. US Army Engineer District-Mobile Mobile United States, 2016.

[6] GRIFFITHS D J, WICKS A. High speed high dynamic range video[J].*IEEE Sensors Journal*, 2017, **17**(8): 2472-2480.

[7] COSSIO T, SLATTON K C, CARTER W, *et al*. Predicting topographic and bathymetric measurement performance for low-SNR airborne lidar[J]. *IEEE Transactions on Geoscience and Remote Sensing*, 2009, **47**(7): 2298-2315.

[8] LIN W T, SHIH P T Y, CHEN J C, *et al*. Bathymetric LiDAR green channel derived reflectance: an experiment from the dongsha 2010 mission[J]. *Terrestrial, Atmospheric & Oceanic Sciences*, 2016, **27**(4): 565-576.

[9] SAYLAM K, BROWN R A, HUPP J R. Assessment of depth and turbidity with airborne Lidar bathymetry and multiband satellite imagery in shallow water bodies of the Alaskan North Slope[J]. *International Journal of Applied Earth Observation and Geoinformation*, 2017, **58**: 191-200.

[10] EREN F, PE′ERI S, RZHANOV Y. Airborne Lidar Bathymetry (ALB) waveform analysis for bottom return characteristics[C]. SPIE Defense+ Security. International Society for Optics and Photonics, 2016: 98270H-98270H-6.

[11] BIRKEBAK M. Airborne lidar bathymetry beam diagnostics using an underwater optical detector array[D]. University

of New Hampshire, 2017.

[12] KOTILAINEN A T, KASKELA A M. Comparison of airborne LiDAR and shipboard acoustic data in complex shallow water environments: Filling in the white ribbon zone[J]. *Marine Geology*, 2017, **385**(1): 250-259.

[13] MOHAMED H, SALAH M, NADAOKA K, *et al*. Assessment of proposed approaches for bathymetry calculations using multispectral satellite images in shallow coastal/lake areas: a comparison of five models[J]. *Arabian Journal of Geosciences*, 2017, **10**(2): 42.

[14] ABDALLAH H, BAGHDADI N, BAILLY J S, *et al*. Wa-LiD: A new LiDAR simulator for waters[J]. *IEEE Geoscience and Remote Sensing Letters*, 2012, **9**(4): 744-748.

[15] ABADY L, BAILLY J S, BAGHDADI N, *et al*. Assessment of quadrilateral fitting of the water column contribution in Lidar waveforms on bathymetry estimates[J]. *IEEE Geoscience and Remote Sensing Letters*, 2014, **11**(4): 813-817.

[16] ABDALLAH H, BAILLY J S, BAGHDADI N N, *et al*. Potential of space-borne LiDAR sensors for global bathymetry in coastal and inland waters[J]. *IEEE Journal of Selected Topics in Applied Earth Observations and Remote Sensing*, 2013, **6**(1): 202-216.